Highly Efficient Luminescent Organic Clusters with Quantum Dot-Like Properties

Chaobin He,* Yang Xiao, Junchao Huang, Tingting Lin, Khine Y. Mya, and Xinhai Zhang

Institute of Materials Research and Engineering, 3 Research Link, Singapore 117602

Received January 20, 2004; E-mail: cb-he@imre.a-star.edu.sg

Quantum dots (QDs) have attracted considerable interest due to the trend toward miniaturization in device-oriented manufacturing.[1] The unique optical and transport properties of QDs have offered great promise in the development of extremely low-threshold laser diodes,[2] biodetectors,[3] single-electron logic devices,[4] and optical computing quantum units.[5]

However, fabrication of stable QDs (currently only inorganic QDs have been reported) presents a formidable challenge because the small dimensions are at the limit of semiconductor-processing techniques. The considerable inhomogeneous line broadening due to the dot size distribution also poses limitations for device applications.[6]

Organic synthesis could provide a routine preparation method which can tailor the properties of materials by structure modification as well as size manipulation. Organic semiconductors with reduced dimensionality are of growing interest, owing to their unique features compared to those of the inorganic semiconductors. Defect-free heterostructures can be more readily fabricated due to weak van der Waals interactions between molecules. The smaller dielectric constants of organic molecules compared to those for inorganic semiconductors could result in strong Coulombic interactions between electrons and holes, leading to large exciton binding energies.[7] However, despite many theoretical studies which predicted quantum confinement effects in heterostructured organic semiconductors,[8] clear experimental observation in one dimension (1D) by multilayer structure[9] and two dimensions (2D) by diluting polymer from bulk material to single chain[10] have just been reported. One major experimental difficulty is the small exciton Bohr radii (a_B) in bulk organic semiconductors ($a_B \approx 1.2-2.0$ nm) which places severe limitations on suitable techniques for preparing the nanoscale structures.[11]

In this communication we report a bottom-up synthesis approach to obtain organic cluster materials in which organic short chains [shorter than exciton Bohr radii (a_B)] were spatially isolated in bulk solid state. The quantum confinement effects in organic chains have been confirmed by the discrete energy levels which are identical to calculations from PLE, narrow PL line, Raman peak red-shift and broadening (compared to the bulk material of chains), size effect from UV, cluster size similar to calculations from TEM, which are typical features of quantum dots.[12]

The organic cluster consists of a cubical core and organic short arms stretched from eight corners of the core. The core structure functions as a stable spacer for separating organic arms to achieve quantum confinement effects. Incorporating the small organic chains onto the cubical core could also prevent phenyl rings from aggregation. The polyhedral oligosilsesquioxane (POSS) is selected as the core due to its rigid cagelike structure and nanoscale dimension (0.53 nm) as well as excellent thermal and mechanical stabilities.[13] The special considerations for using POSS here include its low dielectric constant ($\sim$2.7)[14] and its high band gap (intensive absorption at 6 eV and emission at 4.2 eV)[15] which is much higher

Scheme 1. Molecular Structure of Organic QD Cluster Materials (**G**, **H**), Single Arms (**A**, **B**), Monomers (**C**, **D**, **F**), and POSS (**E**)
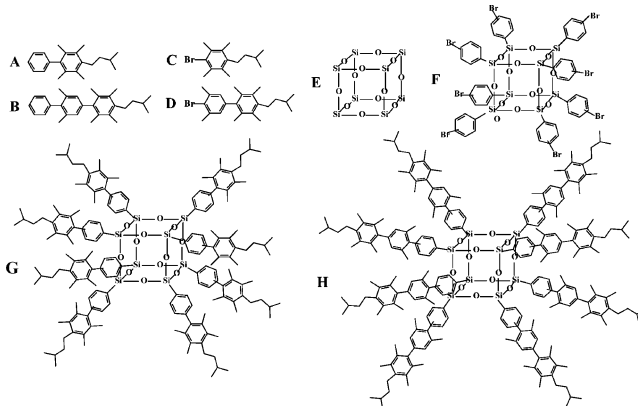
than those of conventional organic compounds or oligomers. These properties make POSS an ideal candidate for isolating organic arms while limiting the influence of electronic properties of POSS on organic moieties. The organic arms work as luminescent centers which are end-capped by alkyl chains to prevent intermolecular aggregation. To minimize the rotating of phenyl rings, which could cause PL line broadening, methyl groups are grafted in each α position of the adjacent phenyl ring to increase the torsion energy barrier.

The cluster materials, denoted as **G** and **H** in Scheme 1, were synthesized via palladium-catalyzed coupling between **C**, **D**, and **F**. It is worth mentioning that the low PL quantum yields[16] η for **A** (7%) and **B** (14%) have been surprisingly increased to those of **G** (33%) and **H** (69%) for thin films after incorporating with POSS. Another notable fact is that **G** and **H** have higher η in solid state than in any solution, which provides proof of intrinsic quantum confinement effects in **G** and **H** because dilution normally increases η for any aggregated system.[10]

The optical properties have been investigated at room temperature for the thin films of **A**, **B**, **G**, and **H** as shown in Figure 1. For comparison the PLE spectrum of unsubstituted biphenyl and triphenyl are also shown in the figure. These two oligophenylenes show unsplit and wider PLE peaks due to the aggregation from $\pi-\pi$ stacking of molecules. **A** and **B** are partially isolated from each other by alkyl chains substituted on one side of oligophenylenes, and as a result, their PLE becomes narrower and discrete to some extent. The organic short chains in **G** and **H** are almost spatially isolated so that the peaks become sharper and discrete. The fwhm of main PLE and PL peaks for **G** and **H** are all less than 10 nm. The spectrum also indicates that the emissive center in **G** and **H** originates from arm **A** and **B** instead of POSS due to the similarity in their PLE spectrum. Different from inorganic QD,[16] the relationship between band gap and size is not following the same formula for organic QDs. The band gap for the organic molecule is more dependent on the structure and composition than
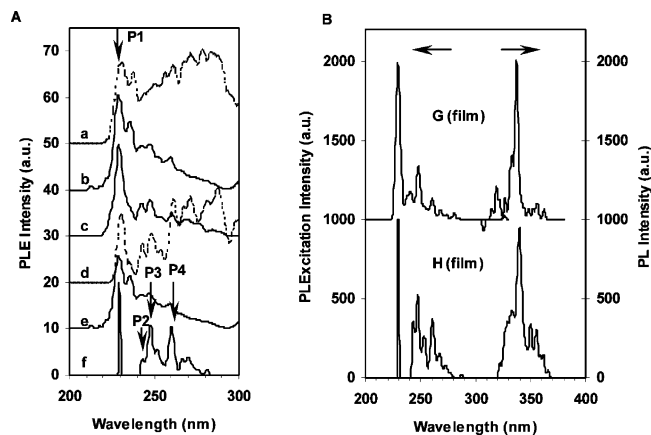
Figure 1. (A) Normalized PLE spectrum of thin film of a: biphenyl, b: material **A**, c: material **G**, d: triphenyl, e: material **B**, f: material **H**. (B) Normalized PL and PLE of material **G** and **H**.

Figure 2. (Left): Modeling of molecular orbital for material **G**, H4 is the fourth-highest occupied orbital, L2 is the second-lowest unoccupied orbital, 1π and $1\pi^*$ are the first ring π and π^* orbital. (Right): TEM image of material **H**.

Table 1. Peak Assignment of PLE Spectrum of **A**, **B**, **G**, **H**[a]

	A		**G**		**B**		**H**	
	Orb. Ph.	Exp. cal.	Orb. Ph.	Exp. cal.	Orb. Ph.	Exp. cal.	Orb. Ph.	Exp. cal.
P1	H3-L3	228	H3-L3	229	H6-L4	229	H5-L4	230
	$1\pi-2\pi^*$	228	$1\pi-2\pi^*$	228	$1\pi-2\pi^*$	229	$1\pi-2\pi^*$	230
P2	H4-L2	242	H4-L2	242	H4-L5	242	H3-L5	243
	$1\pi-1\pi^*$	242	$1\pi-1\pi^*$	239	$2\pi-3\pi^*$	242	$2\pi-3\pi^*$	242
P3	H3-L2	248	H3-L2	248	H5-L2	248	H5-L2	248
	$1\pi-2\pi^*$	248	$1\pi-2\pi^*$	250	$1\pi-1\pi^*$	248	$1\pi-1\pi^*$	248
P4	H2-L4	259	H2-L4	260	H2-L6	259	H2-L6	260
	$2\pi-2\pi^*$	258	$2\pi-2\pi^*$	259	$3\pi-3\pi^*$	257	$3\pi-3\pi^*$	259

[a] Unit: Orb.: molecular orbital, Exp.: wavelength (nm) from experiment result, cal.: wavelength (nm) from modeling, Ph.: phenyl ring, P1: peak1, H1: HOMO, H2: the second-highest occupied molecular orbital, L1: LUMO, L2: the second-lowest unoccupied molecular orbital, 1π:: π orbital of the first phenyl ring (starting from POSS in **G**, **H**), $1\pi^*$: π^* orbital of the first phenyl ring (starting from POSS in **G**, **H**).

on the size. UV spectra for **G** and **H** indicate a slight red-shift when the molecular size increases from **G** to **H**.

Modeling simulation has been conducted, and we conclude: (1) The optimized structure of torsion angle between substituted phenyl rings is around 81°; (2) the orbitals near the highest occupied molecular orbital (HOMO) and the lowest unoccupied molecular orbital (LUMO) (inclusive) for these materials are localized on each arm;[18] (3) the high dihedral angle between phenyl rings makes the molecular orbital (near HOMO and LUMO) contributed almost by single phenyl rings; (4) by substituting phenyl rings at only one corner or at all eight corners of POSS, the energy levels and band gaps are almost same, similar to results in our previous work.[18]

The PL λ_{max} from simulation and experiment are similar for **G** (334 nm) and **H** (340 nm), which means that the majority of arms are essentially equivalent. The identity of excitation wavelength from modeling and experiment could give a clear peak assignment for PLE spectrum of the materials, as shown in Table 1. An example of molecular orbital shape is also shown in Figure 2. From Table
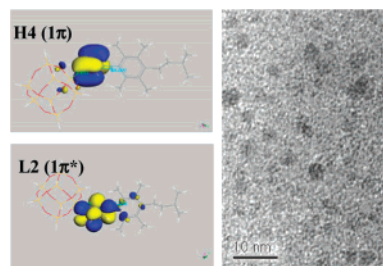
1 we find that P1 (229 nm) in the PLE spectrum is due to excitation from the first phenyl ring (nearest to POSS) π orbital (1π) to the second ring π^* orbital ($2\pi^*$); this peak becomes sharper from **A** to **G** and **B** to **H** because the excitons in the first ring are well confined after the incorporation of the short chains with POSS.

We have studied micro-Raman spectra of **A**, **B**, **G**, **H**. The results indicate that the C−H vibrations from phenyl rings are appreciably red-shifted along with peak broadening. The Raman peak softening and broadening confirm the existence of QD-like vibrational states in bulk solid phase of **G** and **H**.

In summary we report the first organic-based QD cluster materials. The most commonly used method for identifying the quantum confinement effect for inorganic QD (TEM, UV, PL, Raman) have been conducted on these materials, and all of the results indicate these organic cluster materials have QD-like properties.

References

(1) Bukowski, T. J.; Simmons, J. H. *Crit. Rev. Solid State Mater. Sci.* **2002**, *27*, 119.
(2) Fafard, S.; Hinzer, K.; Raymond, S.; Dion, M.; McCaffrey, J.; Feng, Y.; Charbonneau, S. *Science* **1996**, *274*, 350.
(3) Chan, W. C. W.; Nie, S. *Science* **1998**, *281*, 2016.
(4) Nakajima, F.; Miyoshi, Y.; Motohisa, J.; Fukui, T. *Appl. Phys. Lett.* **2003**, *83*, 2680.
(5) Spilller, T. P. *Proc. IEEE* **1996**, *84*, 1719.
(6) Julien, F. H.; Alexandrou, A. *Science* **1998**, *282*, 1429.
(7) Jenekhe, S. A.; Chen, X. L. *Polym. Prepr.* **1997**, *38*, 981.
(8) Seel, M.; Liegener, C. M.; Forner, W.; Ladik, J. *Phys. Rev. B* **1988**, *37*, 956.
(9) Al. Efros, L.; Efros, A. L. *Soviet Phys. Semicond.* **1982**, *16*, 772.
(10) Joshi, H. S.; Jamshidi, R.; Tor, Y. *Angew. Chem., Int. Ed.* **1999**, *38*, 2722.
(11) So, F. F.; Forrest, S. R. *Phys. Rev. Lett.* **1991**, *66*, 2649.
(12) Yoffe, D. *Adv. Phys.* **2002**, *51*, 700.
(13) Choi, J.; Harcup, J.; Yee, A. F.; Zhu, Q.; Laine, R. M. *J. Am. Chem. Soc.* **2001**, *123*, 11420.
(14) Su, R. Q.; Muller, T. E.; Lercher, J. P. J. A. *Adv. Mat.* **2002**, *14*, 1369.
(15) Azinovic, D.; Cai, J.; Eggs, C.; Konig, H.; Marsmann, H. C.; Veprek, S. *J. Lumin.* **2001**, *97*, 40.
(16) Joshi, H. S.; Jamshidi, R.; Tor, Y. *Angew. Chem., Int. Ed.* **1999**, *38*, 2722.
(17) Efros, A. L.; Efros, A. L. *Soviet Phys. Semicond.* **1982**, *16*, 772.
(18) Ling, T.; He, C.; Xiao, Y. *J. Phys. Chem. B* **2003**, *107*, 13788.

JA049650J